Journal of Alloys and Compounds 690 (2017) 239–248

Contents lists available at ScienceDirect

Journal of Alloys and Compounds

journal homepage: http://www.elsevier.com/locate/jalcom

Influence of oxygen deficiency on the synthesis of tungsten oxide and the photocatalytic activity for the removal of organic dye

Guojuan Hai, Jianfeng Huang*, Liyun Cao**, Yanni Jie, Jiayin Li, Xing Wang, Ge Zhang

School of Materials Science and Engineering, Shaanxi University of Science & Technology, Xi'an 710021, China

ARTICLE INFO

Article history:
Received 11 April 2016
Received in revised form
11 August 2016
Accepted 13 August 2016
Available online 15 August 2016

Keywords:
Tungsten oxide
Flower-like structure
Photoelectrochemical
Oxygen vacancy
Photocatalytic activity

ABSTRACT

Self-assembly flower-like $WO_3/W_{18}O_{49}$ and $W_{18}O_{49}$ were synthesized through a facile solvothermal method. By reducing the content of oxygen, the phase of $WO_3/W_{18}O_{49}$ changes to pure $W_{18}O_{49}$ and the morphology of the $W_{18}O_{49}$ shows an obvious evolution from nanowire to flower-like $W_{18}O_{49}$ assembled by nanoneedle. The crystallite size of $WO_3/W_{18}O_{49}$ and $W_{18}O_{49}$ are 29.85 nm and 14.13 nm, respectively. The photocatalytic activity of $W_{18}O_{49}$ UV-light irradiation is about 8 times as high as that of $WO_3/W_{18}O_{49}$. This enhanced activity is attributed to smaller crystallite size and larger surface area. Furthermore, XPS analyses reveal that the lattice oxygen reduces under N_2 atmosphere. The increasing of oxygen vacancy results in a narrowing bandgap and strong light absorption performance. By combining the results of the transient photocurrent and electrochemical impedance measurements, the electron-hole pair separation rates and carrier migration rates of the $W_{18}O_{49}$ have been greatly improved.

1. Introduction

Free and abundantly available solar light is a clean, safe and renewable source of energy. Photocatalysis technology is a desirable method for energy generation and wastewater treatment because it is an inexpensive and convenient [1]. It can totally decompose dye molecules into inorganic small molecules. Numerous studies related to the photocatalytic performance of oxide semiconductor have been carried out. As one of the important n-type semiconductors, tungsten oxides (WO_x, $x = 1–3$) have been extensively investigated for lithium-ion batteries [2], gas sensors [3], supercapacitive performance [4], photocatalysis [5]. Among the $WO_{2.625}$-WO_3, monoclinic $W_{18}O_{49}$ ($WO_{2.72}$) has the largest amount of oxygen vacancies which can act as traps and tightly catch reactant molecules [6]. Moreover, the $W_{18}O_{49}$ has been reported as the only oxide that can exist in a pure form [7]. Especially, because of the distinctive defect structure and broad absorption extending to near infrared (NIR) regions, $W_{18}O_{49}$ has been extensively studied [8].

However, the $W_{18}O_{49}$ is easily oxidized to WO_3 under the condition of elevated temperature [9]. It is found that the W surface has the lowest oxidization degree when the concentration of oxygen is low. Therefore, we conclude that reducing the content of oxygen will be conducive to the synthesis of the non-stoichiometric $W_{18}O_{49}$ in the process of solvothermal reaction. Particularly, $W_{18}O_{49}$ has strong anisotropic growth behavior along the [010] direction, and this feature easily results in the formation of one-dimensional form, such as nanowires, nanorods, nanobundles [10–13]. So it still remains a significant challenge to develop a facile method to organize well-defined 2D or 3D morphology-controlled $W_{18}O_{49}$ microstructures with more oxygen deficiencies and better performance.

In the present work, we report a simple approach to actualizing 3D tungsten oxide materials without any assistant agents. When the sample prepared under N_2 atmosphere, the flower-like $W_{18}O_{49}$ has been obtained through the solvothermal method. It is organized by 2D nanostructure. The change of the crystal phase and the morphology evolvement are expounded in detail. In addition, some electrochemistry means have been introduced to assist the influence of the oxygen vacancies on the improved photocatalytic performance.

2. Experimental

2.1. Synthesis of samples

All of the reagents were analytical grade. At first, 0.7931 g of

* Corresponding author.
** Corresponding author.
E-mail addresses: huangjfsust@126.com (J. Huang), 2644245930@qq.com (L. Cao).

http://dx.doi.org/10.1016/j.jallcom.2016.08.099
0925-8388/

WCl_6 (0.05 M) was dissolved in 40 ml of absolute ethanol to form a pale yellow solution. After constantly magnetic stirring for 30 min under air atmosphere condition, the dark blue solution was observed. This blue solution was kept with sonication for 10 min, after which it was transferred into a 100 ml Teflon-lined autoclave. In order to reduce air content in the Teflon-lined autoclave as much as possible, this process was conducted in the glove box so that the 100 ml Teflon-lined autoclave was filled with enough N_2. The solvothermal reaction was conducted at 160 °C for 24 h. After that, the autoclave was cooled naturally to room temperature. The final products were centrifuged and washed by ethanol for several times to remove ions and organic residues, followed by vacuum drying at 60 °C, 5 h. Then blue flocculating precipitates were collected. As a comparison, we did an another experiments without in the glove box and no N_2 treatment.

2.2. Characterization of samples

The phase composition of the samples were characterized by a powder X-ray powder diffractometer (XRD, Rigaku D/max-2200 PC) with Cu Ka radiation ($\lambda = 1.5406$ Å). The morphology and structure were determined by scanning electron microscopy (FE-SEM, S-4800, Hitachi, Japan) and a transmission electron microscope (TEM, TecnaiG2F20S-TWIN). The chemical states and ion ratios of the surface were investigated by X-ray photoelectron spectroscopy (XPS, Thermo ESCALAB 250). Brunauer emmet teller (BET) surface areas were characterized with the nitrogen adsorption method on the Micromeritics 3020 instrument. The UV–vis diffuse reflectance spectrum (LAMBDA950, PerkinElmer) was used in the wavelength range of 200–800 nm to study the absorption range.

2.3. Photocatalytic evaluation

Methyl orange (MO) was adopted as a typical pollutant to evaluate the photocatalytic activity of the as-prepared products. 50 mg of the photocatalyst was added to 50 mL MO solution (10 mg L^{-1}) and dispersed under ultrasonic vibration for 5 min. Before light irradiation, the suspension was magnetically stirred in darkness for 90 min to achieve an absorption-desorption equilibrium. A 300 W Hg lamp and 500 W xenon lamp were used as the light source, which was conducted in an BL-GHX-V photochemical reactor (Bilon Machine Factory, China). The concentration of MO was determined on a UV–vis spectrophotometer (Unico, UV-2600) by monitoring its characteristic absorption at 463 nm.

2.4. Photoelectrochemical measurements

Photoelectrochemical measurements were carried out using a three-electrode quartz cell on the CHI-660B electrochemical system. The platinum wire is the counter electrode and the saturated calomel electrode (SCE) is the reference electrode. The tungsten oxide film electrodes were suspended in the 0.5 mol L^{-1} Na_2SO_4 aqueous electrolyte as working electrodes. All the photoelectrochemical measurements were performed under a UV light source (CEL-HXUV300, 200–400 nm) and visible light source (wavelength range of 400–700 nm). Electrochemical impedance spectra (EIS) were obtained in the frequency range of 0.01–100000 Hz and then interpreted by a nonlinear least-squares fitting procedure using a commercial software (ZsimpWin).

3. Results and discussion

Fig. 1a displays the XRD pattern of the sample prepared by solvothermal method without N_2 treatment. It gives rise to similar XRD pattern of triclinic WO_3 phase (JCPDS Card no. 24-0747). It is easy to find that the (010) plane of $W_{18}O_{49}$ (JCPDS Card no. 71-2450) is close to the XRD diffraction pattern of the triclinic WO_3 phase (JCPDS Card no. 24-0747). And an additional diffraction peak indicated by the circle in Fig. 1a is found. It is consistent with the (020) plane of the $W_{18}O_{49}$ (JCPDS Card no. 71-2450). So, It is hard to determine the crystal phase using the XRD data alone [14]. X-Ray diffraction of the sample prepared under N_2 atmosphere condition is shown in Fig. 1b. It indicates that the product is unambiguously assigned to the monoclinic phase $W_{18}O_{49}$ with lattice constants of $a = 18.334$ Å, $b = 3.786$ Å, $c = 14.044$ Å, and $\beta = 115.20°$ (JCPDS Card no. 71-2450). The relatively intense diffraction peaks locating at 27.00° and 49.35° corresponding to the (010) and (020) planes.

The morphology and microstructure of the samples prepared without N_2 treatment were examined by SEM and TEM. In Fig. 2a and b, numerous nanosheets are assembled to form three-dimensional (3D) flower-like structure with a diameter about 2.5 μm. As shown in Fig. 2b, these building blocks contain a majority of nanowires, which merge with "petals" closely. The TEM image in Fig. 2c shows the outline of a typical flower-like structure. The corresponding selected area electron diffraction (SAED) pattern of nanosheet was taken from the area marked in red in Fig. 2d, which can be indexed to the diffraction planes of (020), (220) and (040) for the triclinic WO_3 phase (JCPDS Card no. 24-0747). A magnified image of the edge was taken in Fig. 2e. It exhibits several nanowires cross each other on the edge. It is in accordance with the SEM observation. In order to further analyze the composition of nanowires on the flower-like structure. Fig. 2f presents the high-resolution transmission electron microscopy (HRTEM) image of the nanowires with the diameter about 10–13 nm. The lattice spacing along (010) is determined to be 0.378 nm, in agreement with the reported lattice constant of monoclinic $W_{18}O_{49}$ [15]. So it can be concluded that the nanowires belong to $W_{18}O_{49}$. The formation of WO_3 flower-like hierarchical architectures may be attributed to the Ostwald ripening process and self assembly process [16]. The $W_{18}O_{49}$ nanowires are closely integrated with the flower-like structure. It is because of the following reasons: $W_{18}O_{49}$ contains some defects intrinsically, such as shear planes, oxygen vacancies and stacking faults, which may favor the formation of this tightly structure during solvothermal synthesis [17]. On the other hand, the formation of the tightly structure is the result of the hydrogen bonding interaction and the large surface energy between the thinner nanowires and flower-like structure [18,19]. Together with the XRD and TEM results, it can be concluded that

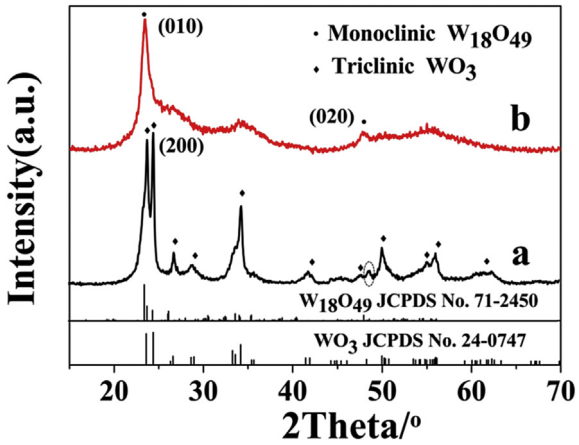

Fig. 1. XRD patterns of (a) as-synthesized $WO_3/W_{18}O_{49}$ by solvothermal method without N_2 treatment and (b) $W_{18}O_{49}$ prepared under N_2 atmosphere condition.